Applications of Data-Selective Adaptive Filters

Markus V. S. Lima, Breno N. Espíndola, Fábio P. Freeland and Paulo S. R. Diniz

***Resumo*— Neste artigo nós discutimos sobre as potencialidades e importância de mecanismos de seleção de dados em problemas reais. Nós mostramos como filtros adaptativos com seletividade de dados podem ser explorados com a finalidade de melhorar o desempenho de sistemas de comunicações e canceladores de eco acústico. Para sistemas de comunicações propomos algoritmos com seletividade de dados para equalização semi-cega em sistemas baseados em OFDM empregando o esquema de modulação digital QPSK que aumenta o *throughput* do sistema em 18%, desde que uma razão-sinal-ruído mínima seja garantida. Para o cancelamento de eco acústico propomos algoritmos com seletividade de dados que operam no domínio da frequência e possibilitam uma redução significativa da carga computacional. Os resultados de simulações mostram que, após a convergência, esses algoritmos atualizam apenas 10% dos coeficients do filtro.**

***Palavras-Chave*— Filtros adaptativos com seletividade de dados, equalização semi-cega, OFDM, cancelamento de eco acústico.**

***Abstract*— In this article we discuss the capabilities and importance of data selection mechanisms in real-world tasks. We show how data-selective adaptive filters can be explored in order to improve the performance of communication systems and acoustic echo cancellers. For communications systems we propose a data-selective algorithm for semi-blind equalization in OFDM-based systems employing a QPSK digital modulation scheme that increases in 18% the system throughput, provided a minimum signal-to-noise ratio is guaranteed. For the acoustic echo cancellation we propose data-selective algorithms that operate in the frequency domain and allow a significant reduction of the computational burden. The simulation results show that after convergence, these algorithms update only 10% of the filter coefficients.**

***Keywords*— Data-selective adaptive filters, Semi-blind equalization, OFDM, acoustic echo cancellation.**

I. Introduction

In recent years, mainly due to the decreasing prices of sensors and storage devices, we have been witnessing an enormous increase in the amount of data to be processed and/or stored. For instance, multiple antennas are being used in communications systems to increase system capacity, multiple microphones are being used in multimedia applications like audio enhancement and localization of a sound source, as well as databases are getting bigger.

In this complex scenario, data-selective filters can be regarded as tools for automatic evaluation/selection of data. These tools have the potential to discard undesired data, such as outliers and redundancy, and to peep a reduced amount of data (filtered data) that is most relevant to the given application.

Data-selective adaptive (DSA) filters are self-adjustable mechanisms whose learning process is based only on filtered data. Among the benefits of discarding data before performing the adaptation of the filter are: 1) Saving computational resources, and thus energy, by not adapting all the time, 2) Better learning performance since undesired artifacts and data with no innovation are removed [1].

This paper presents results of ongoing research on DSA filters applied to the equalization of *orthogonal frequency-division multiplexing* (OFDM) systems and acoustic echo cancellation. For the OFDM system we propose a *semi-blind equalization* (SBE) scheme that has potential to increase system throughput allowing the receiver to track time-varying channels. For the acoustic echo cancellation we propose a frequency-domain data-selective algorithm that yields the same perceived result as the state-of-the-art solutions, but requiring much lower computational power.

This paper is organized as follows. In section II we present the *set-membership filtering* (SMF) paradigm which leads to DSA filters. In sections III and IV we show some applications of DSA filters to communications systems and echo cancellation. In both sections we follow a similar approach: first we explain the application in which a DSA filter has potential to enhance the performance, then we describe the proposed algorithm, and finally we show some simulation results. The conclusions are drawn in section V.

Notation: We denote scalars by lowercase letters, vectors by lowercase boldface letters, and matrices by uppercase boldface letters. All vectors are column vectors. We use $\mathbb{R}$ and $\mathbb{C}$ to denote the real and complex fields respectively, $\mathbb{R}_+$ to denote the set of non-negative real numbers, and the set of natural numbers is represented by $\mathbb{N}$. The point-wise multiplication and division between two vectors of the same size is represented by $\mathbf{a} \circ \mathbf{b}$ and $\mathbf{a} \div \mathbf{b}$. In addition, $\mathrm{diag}\{\mathbf{x}\}$ is a diagonal matrix having $\mathbf{x}$ on its main diagonal.

II. Data-Selective Adaptive Filtering

In general terms, *data-selective adaptive* (DSA) filters are special kinds of adaptive filters that evaluate the amount of information (innovation) present in the input data before using it to self-adjust its coefficients according to an algorithm. The DSA filters bring about robustness against noise and reduced overall computational burden [1]. In the following we present the *set-membership filtering* (SMF) paradigm which has been successfully used to derive powerful data-selective algorithms [2], [3], [4].

The SMF concept appeared in [2] and is applicable to adaptive filtering problems that are linear-in-parameters, i.e., whose input-output signals are related by $y = \mathbf{w}^T\mathbf{x}$, in which $\mathbf{x} \in \mathbb{R}^M$ is the input vector, $\mathbf{w} \in \mathbb{R}^M$ represents the filter coefficients, and the output of the filter is given by y.

According to the SMF criterion, we want to estimate the parameter $\mathbf{w}$ that leads to an error signal $e = d - y$ whose

Markus V. S. Lima, Breno N. Espíndola, Fábio P. Freeland e Paulo S. R. Diniz, Electrical Engineering Program/COPPE, Federal University of Rio de Janeiro, Rio de Janeiro, Brazil, E-mails: {markus,breno,ffreeland,diniz}@lps.ufrj.br. This work was supported by CNPq, CAPES and FAPERJ.

magnitude is upper bounded by a constant $\overline{\gamma} \in \mathbb{R}_+$, for all possible pairs $(\mathbf{x}, d)$, where $d \in \mathbb{R}$ is the desired-output signal. Denoting by $\mathcal{S}$ the set comprised of all possible pairs $(\mathbf{x}, d)$, and defining the *feasibility set* Θ as

$$\Theta = \bigcap_{(\mathbf{x},d)\in\mathcal{S}} \left\{\mathbf{w} \in \mathbb{R}^M : |d - \mathbf{w}^T\mathbf{x}| \leq \overline{\gamma}\right\}, \qquad (1)$$

the SMF criterion consists of finding $\mathbf{w} \in \Theta$.

In practice we do not have access to $\mathcal{S}$, since this would require *a priori* knowledge of all possible input and desired-output signals. Therefore Θ, or a point in it, cannot be directly estimated. However, iterative estimates can be found as we get to know the terms of the sequences $(\mathbf{x}(k), d(k))$, for $k \in \mathbb{N}$.

Defining the *constraint set*

$$\mathcal{H}(k) = \left\{\mathbf{w} \in \mathbb{R}^M : |d(k) - \mathbf{w}^T\mathbf{x}(k)| \leq \overline{\gamma}\right\}, \qquad (2)$$

i.e., the set comprised of all $\mathbf{w}$ satisfying the error bound at iteration k, the feasibility set Θ can be estimated by means of the *exact-membership set*

$$\psi(k) = \bigcap_{i=0}^{k} \mathcal{H}(i). \qquad (3)$$

Fig. 1 depicts the geometrical interpretation of the SMF paradigm. The "size" of $\psi(k)$ decreases for each k in which the pairs $(\mathbf{x}(k), d(k))$ bring some innovation. Thus, for sufficiently large k, Θ can be well approximated by $\psi(k)$.

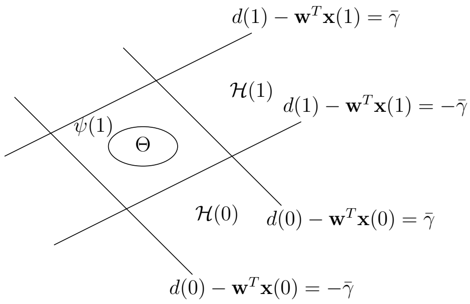

Fig. 1. SMF geometrical interpretation in the parameter space: $\psi(1) = \mathcal{H}(0) \bigcap \mathcal{H}(1)$.

The SMF concept can also be extended to the frequency domain as shown in [4].

III. Application to Communications Systems

In this section we discuss how DSA filters can be applied to communications systems. In fact, we show a data-selective algorithm that can be used as a *semi-blind equalization* (SBE) method for OFDM-based systems employing QPSK digital modulation scheme.

A. OFDM-based Systems

Orthogonal frequency-division multiplexing (OFDM) has been chosen as the modulation scheme of some important communications standards such as the Wi-Fi [5], WiMAX [6], and the downlink connection of the LTE (Long Term Evolution) [7].

In these systems, *reference signals* (also known as *pilots*) are periodically transmitted. The pilots are used at the receiver to perform channel estimation, and this estimate is then used in the equalization process of subsequent OFDM symbols. However, sending pilots decreases the system throughput since no information is actually transmitted. In LTE, for example, a whole OFDM symbol containing only pilots is sent at each 6 or 7 transmitted OFDM symbols, depending on the size of the cyclic prefix.

Blind equalization algorithms can be employed to increase the system throughput, since they do not use pilots. In addition, these algorithms allow tracking of channel variations, which is a useful feature since real channels are usually time-varying, especially the wireless channel. On the other hand, blind algorithms usually require a proper initialization and can lose track in nonstationary environments, deteriorating the channel equalization process.

Semi-blind algorithms represent a trade-off between the gains of using blind equalization techniques and supervised (i.e., pilot-based) schemes. They allow the communication system to send pilots less often, increasing the system throughput while keeping the channel equalization effective. In the following we present an SBE algorithm for channel equalization of OFDM symbols employing QPSK digital modulation scheme.

B. Semi-Blind Equalization Scheme

Fig. 2 illustrates a frequency-domain block representation of an OFDM-based scheme connected to the proposed SBE algorithm. In this figure we considered that the cyclic-prefix length is greater than the channel memory, so that the equivalent channel that modifies the modulated symbols is $\mathbf{h}(k) \in \mathbb{C}^M$, which is the actual channel frequency response. See [9] for further details on the mathematical modeling of OFDM systems.

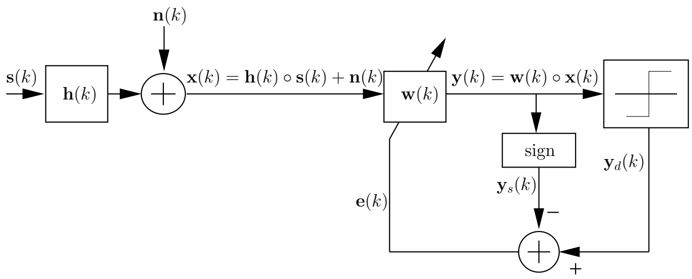

Fig. 2. Frequency-domain representation of an OFDM transmission using the proposed semi-blind equalization scheme at the receiver.

Here, all vectors are in $\mathbb{C}^M$, where M is the number of subcarriers of the OFDM-based system. The kth transmitted OFDM symbol is denoted by $\mathbf{s}(k)$, whose elements are symbols belonging to a QPSK modulation. The M-point *fast Fourier transform* (FFT) of the channel impulse response is represented by $\mathbf{h}(k)$, and $\mathbf{n}(k)$ is the *additive white Gaussian noise* (AWGN) vector with standard deviation σ_n. The input vector $\mathbf{x}(k) = \mathbf{h}(k) \circ \mathbf{s}(k) + \mathbf{n}(k)$ contains the received symbols in the frequency domain, and $\mathbf{w}(k)$ represents the adaptive equalizer coefficients also in the frequency domain. The output vector $\mathbf{y}(k) = \mathbf{w}(k) \circ \mathbf{x}(k)$ contains the equalized received symbols. In addition, $\mathbf{y}_d(k) = \text{QPSK decision}\{\mathbf{y}(k)\}$ contains the QPSK symbols that are most likely to have been transmitted, whereas $\mathbf{y}_s(k) = \text{sign}\{\mathbf{y}(k)\}$ contains the equalized received symbols projected on the unit circle, i.e., each of its elements corresponds to a projection of an element of $\mathbf{y}(k)$ (a complex number) on the unit-radius circle. Since the elements of $\mathbf{y}_d(k)$ are points belonging to a QPSK constellation, we must project the elements of $\mathbf{y}(k)$ on the unit circle (forming $\mathbf{y}_s(k)$) in order to have a decision-direct criterion that does not take into account the modulus of the components of $\mathbf{y}(k)$. The error vector, defined as $\mathbf{e}(k) = \mathbf{y}_d(k) - \mathbf{y}_s(k)$, determines whenever an update in the adaptive filter $\mathbf{w}(k)$ is needed.

TABLE I

SEMI-BLIND EQUALIZATION ALGORITHM.

SBE Algorithm

```
For k = 1:(Number of OFDM symbols) do
{
  Initialization
  {
    Choose δ(k) as a small constant
    Choose γ(k) (usually as a function of σ_n)
  }
  If pilot was sent, then
  {
    Do channel estimation
    Compute the equalizer w_MMSE(k)
    w(k) = w_MMSE(k) / |w_MMSE(k)|
  }
  Else
  {
    y(k) = w(k) ∘ x(k)
    y_s(k) = sign{y(k)}
    y_d(k) = QPSK decision{y(k)}
    e(k) = y_d(k) − y_s(k)
    For m = 1 : M (Number of subcarriers) do
    {
      μ_m(k) = (1 − γ_m(k)/|e_m(k)|)   if |e_m(k)| > γ_m(k)
               0                        otherwise
    }
    w(k+1) = w(k) + μ(k) ∘ [e(k) ÷ (x(k) + δ(k)u)] ∘ |x(k)|
    w(k+1) = w(k+1) / |w(k+1)|
  }
}
```

The SBE algorithm is summarized in Table I. The regularization parameter $\delta(k)$ must be chosen as a small constant used to prevent numerical instabilities due to small values for the entries of $\mathbf{x}(k)$. The vector $\boldsymbol{\gamma}(k) \in \mathbb{R}_+^M$ contains decision thresholds for each subcarrier error, i.e., the algorithm updates only if the modulus of the mth element of $\mathbf{e}(k)$, viz. $|e_m(k)|$, is greater than the corresponding entry of $\boldsymbol{\gamma}(k)$. The vector $\boldsymbol{\mu}(k)$ contains the step-size for each filter coefficient and $\mathbf{u} = \begin{bmatrix}1 & 1 & \dots & 1\end{bmatrix}^T \in \mathbb{R}^M$.

C. Simulation Results

Here, it is assumed that the length of the cyclic prefix is appropriately chosen in such a way that the transmission scheme summarized in Fig. 2 is valid. The simulation setup follows closely the configuration of the physical-layer downlink connection of the LTE system [7]. Each OFDM symbol is comprised of $M = 512$ subcarriers, each subcarrier corresponding to 15 kHz carries one symbol belonging to a QPSK constellation whose symbols are normalized to have unity variance. The channel is time varying. For the first OFDM symbol of each simulation, the channel $\mathbf{h}(0)$ is generated according to the Extended Typical Urban-LTE (ETU-LTE) model [8]. The channels observed by the other OFDM symbols were generated following a *random-walk model* [1] applied only to the phase of the frequency response of the channel, i.e.,

$$\begin{aligned}
\mathbf{h}(k) &= |\mathbf{h}(k)|e^{j\boldsymbol{\theta}(k)}, \\
\mathbf{h}(k+1) &= |\mathbf{h}(k)|e^{j\boldsymbol{\theta}(k+1)}, \\
\boldsymbol{\theta}(k+1) &= \lambda_c\boldsymbol{\theta}(k) + \kappa\mathbf{n}_c(k),
\end{aligned} \tag{4}$$

where $\mathbf{h}(k)$ is the frequency response of the channel during the kth OFDM symbol, $|\mathbf{h}(k)|$ and $\boldsymbol{\theta}(k)$ are vectors containing the modulus and the phase components, respectively, of $\mathbf{h}(k)$. The other parameters are $\lambda_c = 0.99$, $\kappa = (1-\lambda_c)^{p/2}$, $p = 2$, and $\mathbf{n}_c(k)$ is a random vector drawn from a zero-mean Gaussian distribution with standard deviation $\sigma_{n_c} = 5$.

The bit-error rate (BER) results were generated considering 10^4 transmitted OFDM symbols and then averaging the results over 100 independent simulations.

Fig. 3 summarizes the BER results for different values of signal-to-noise ratio (SNR) considering a channel that varies at every OFDM symbol. The channel frequency response modulus is constant for each simulation and it was generated in such a way that it's minimum value is 0.5. This particularization on the channel is justified by our SBE process, which is very sensible to the *SNR at a given subcarrier*. Indeed, from the transmission scheme we know that the symbol received at the mth subcarrier is given by $x_m(k) = h_m(k)s_m(k) + n_m(k)$, and the *SNR at this subcarrier* is given by $|h_m(k)s_m(k)|^2/|n_m(k)|^2$, and thus, for low values of $|h_m(k)|^2$ we might have a signal power much lower than the noise power at the receiver.

Fig. 3 also shows that the SBE algorithm can dramatically increase the system capacity provided a minimum SNR is guaranteed. For instance, at an SNR of 20 dB, the SBE scheme that transmits a pilot OFDM symbol at every 60 OFDM symbols achieves almost the same BER as of the traditional OFDM retransmitting pilot OFDM symbols at each 6 OFDM symbols. In this case, the usage of the SBE technique would yield an increase of 18% in the throughput as compared to the traditional OFDM transmission.

IV. APPLICATION TO ECHO CANCELLATION

In this section we discuss how DSA filters can be applied to address the well-known echo cancellation problem. We present a data-selective algorithm that operates in frequency

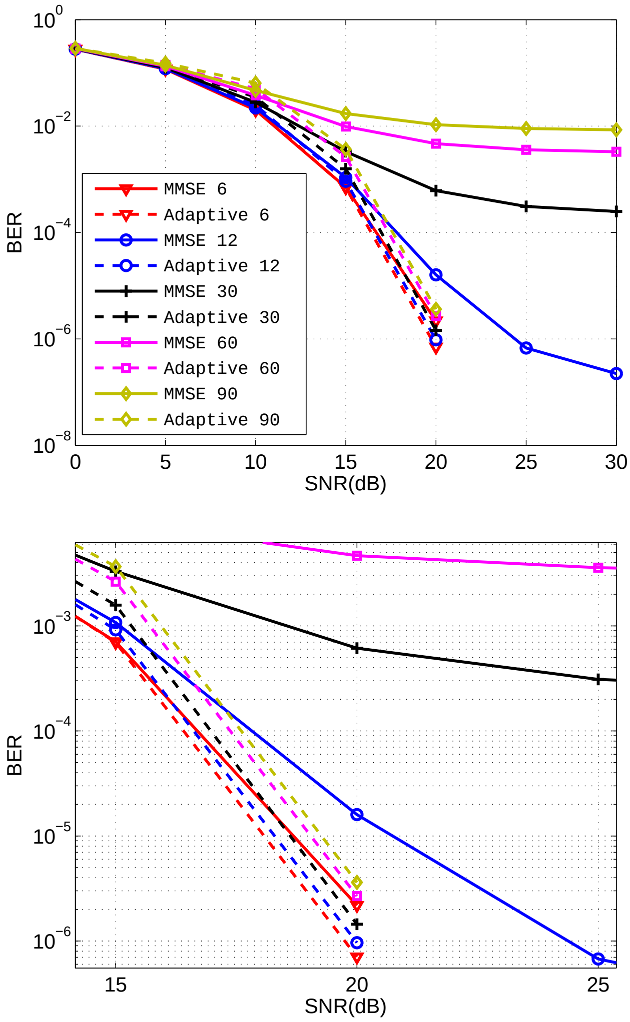

Fig. 3. BER versus SNR. In the first plot (top) we consider $|h_m(k)| > 0.5$ for all m (subcarriers) and k (OFDM symbols), whereas the second plot (bottom) is just a zoom of the previous one.

domain and obtains a significant reduction in the computational burden, as compared to the typical algorithms used for this application.

A. Acoustic Echo Cancellation

Acoustic echo appears when there exists an acoustic coupling between loudspeaker(s) and microphone(s), e.g., in hands-free communications and teleconference systems. The state-of-the-art solution to this problem is to use an acoustic echo canceller based on simple adaptive filters, such as the LMS and BNLMS [10]. The inconvenient is that such an application usually requires long-length adaptive filters and, consequently, more computational power and latency as compared to the short-length counterparts [1], [10].

B. Frequency-Domain DSA Filter

In Table II we summarize the proposed Frequency-Domain DSA algorithm. This algorithm is based on the Constrained Frequency-Domain algorithm [1], but it incorporates the SMF criterion in order to benefit from the data selection.

In this algorithm, γ is a regularization factor used to avoid ill-conditioning of the matrix $\mathbf{\Sigma}$, $(1-\alpha)$ can be seen as a forgetting factor for the variance $\sigma_k^2(m)$ of $u_k(m)$, $\mathbf{x}(m) \in \mathbb{R}^L$ is the input-signal vector, $\mathbf{I}_L$ and $\mathbf{0}_L$ stand for the identity and all-zero matrices of size L, $\mathbf{F}_{2L}$ represents the unitary Discrete-Fourier-Transform (DFT) matrix of length $2L$. In addition, $\mathbf{u}(m) \in \mathbb{C}^{2L}$ represents the DFT of two concatenated input-signal vectors $\mathbf{x}(m)$ and $\mathbf{x}(m-1)$. The vectors $\mathbf{d}(m), \mathbf{y}(m), \mathbf{e}(m) \in \mathbb{C}^L$ are, respectively, the desired-output signal, output signal, and error signal in time domain, whereas $\tilde{\mathbf{e}}(m) \in \mathbb{C}^{2L}$ is the DFT of $\mathbf{e}(m)$ padded with zeros. μ_k is the convergence factor (step size) relative to the kth FFT bin, $\mathbf{\Lambda}$ is a diagonal matrix whose nonzero entries are given by the convergence factors. $\mathbf{W}(m) \in \mathbb{C}^{2L}$ is an auxiliary variable that represents the unconstrained frequency-domain adaptive filter, whereas $\mathbf{W}_c(m) = [w_{c,0}, w_{c,1}, \ldots, w_{c,2L-1}]^T \in \mathbb{C}^{2L}$ contains the taps of the constrained frequency-domain adaptive filter.

Γ_k represents the upper bound in which the magnitude of the error corresponding to the kth bin, namely $|\tilde{e}_k(m)|$, is acceptable, i.e., no update is performed for errors lower than Γ_k. The threshold $\check{\Gamma}_k$, usually chosen as a function of the noise standard deviation, determines the level of residual error that will be left in the filter output.

We have been working mainly with two variations of the SM-CFD algorithm. In both of them $\check{\Gamma}_k$ is chosen as a fixed value for all k (bins). In the first variation, called Fixed-SM-CFD (F-SM-CFD), Γ_k is also a fixed value given by $\Gamma_k = \check{\Gamma}_k$. In the second one, called Perceptual-SM-CFD (P-SM-CFD) we choose Γ_k according to some psychoacoustic criteria, such as *masking* and *just-noticeable changes* [11]. The idea is that we should not bother with residual errors that we cannot hear.

C. Simulation Results

In order to evaluate the quality of the echo cancellers, a set of 24 signals was prepared. Each of the signals was generated by concatenating distinct phonetic-balanced sentences [12] with a silence gap between them as recommended in [13]. The sentences are in Brazilian Portuguese and were recorded by native people (2 males and 1 female) and the duration of the 24 signals varies from 100 to 170 seconds.

Then, these signals were contaminated with acoustic echo using gain levels of $\{-20, -30, -40, -50\}$ dB with respect to the reference signal, and delay values of $\{50, 100, 150, 200, 250, 300\}$ ms, in all possible combinations. The contamination model includes the far-end room-impulse responses (RIRs) which were randomly chosen from a set of RIRs obtained from [14], [15]. In the sequence, white Gaussian noise was added to the signal filtered by the RIR. The white-noise power was such that the SNR levels were randomly chosen as $\{30, 40, 50\}$ dB with respect to level of echo signal.

Fig. 4 illustrates the dramatic saving in computational power, and thus energy, that the SM-CFD algorithm can yield, especially after its convergence. For instance, in average, for the 60th block the F-SM-CFD algorithm updated only 10% of its taps, and the P-SM-CFD algorithm updated only 4% of its taps. Recalling that L is usually large for acoustic echo cancellation, this reduction on the number of updates per block is

TABLE II
SET-MEMBERSHIP CONSTRAINED FREQUENCY-DOMAIN (SM-CFD) ALGORITHM.

SM-CFD Algorithm

Initialization
{
Choose γ as a small constant
Choose α such that $0 < \alpha \leq 0.1$
Compute M (number of blocks of length L to be processed)
$\mathbf{x}(0) = \mathbf{0}$
$\sigma_k^2(0) = 0$, for $k = 1, 2, \cdots, 2L$
}
For $m = 1{:}M$ (i.e., for each block of length L) do
{

$$\mathbf{u}(m) = \mathbf{F}_{2L} \begin{bmatrix} \mathbf{I}_L \\ z^{-1}\mathbf{I}_L \end{bmatrix} \mathbf{x}(m) = \mathbf{F}_{2L} \begin{bmatrix} \mathbf{x}(m) \\ \mathbf{x}(m-1) \end{bmatrix}$$

$$\mathbf{y}(m) = [\mathbf{I}_L \;\; \mathbf{0}_L]\, \mathbf{F}_{2L}^H \begin{bmatrix} w_{c,0}(m)u_0(m) \\ w_{c,1}(m)u_1(m) \\ \vdots \\ w_{c,2L-1}(m)u_{2L-1}(m) \end{bmatrix}$$

$$\mathbf{e}(m) = \mathbf{d}(m) - \mathbf{y}(m)$$

$$\tilde{\mathbf{e}}(m) = \mathbf{F}_{2L} \begin{bmatrix} \mathbf{I}_L \\ \mathbf{0}_L \end{bmatrix} \mathbf{e}(m)$$

For $k = 1{:}2L$ (i.e., for each bin) do
{
Compute Γ_k and $\breve{\Gamma}_k$ according to the type of the SM-CFD

$$\mu_k = \begin{cases} \frac{1}{8}\left(1 - \dfrac{\breve{\Gamma}_k}{|\tilde{e}_k(m)|}\right) & \text{if } |\tilde{e}_k(m)| > \Gamma_k \\ 0 & \text{otherwise} \end{cases}$$

$$\sigma_k^2(m) = (1-\alpha)\sigma_k^2(m-1) + \alpha |u_k(m)|^2$$

}

$$\mathbf{\Lambda}(m) = \mathrm{diag}\left(\mu_1, \mu_2, \cdots, \mu_{2L}\right)$$

$$\mathbf{\Sigma}^2(m) = \mathrm{diag}\left(\gamma + \sigma_1^2, \cdots, \gamma + \sigma_{2L}^2\right)$$

$$\mathbf{W}(m+1) = \mathbf{W}(m) + 2\mathbf{\Lambda}(m)\mathbf{\Sigma}^{-2}(m)\mathrm{diag}\left(\tilde{\mathbf{e}}(m)\right)\mathbf{u}^*(m)$$

$$\mathbf{W}_c(m+1) = \mathbf{F}_{2L}^H \begin{bmatrix} \mathbf{I}_L \\ \mathbf{0}_L \end{bmatrix} [\mathbf{I}_L \;\; \mathbf{0}_L]\, \mathbf{F}_{2L}\mathbf{W}(m+1)$$

}

impressive. In addition, since the proposed adaptive algorithm operates in the frequency domain, as opposed to the traditional algorithms that are usually employed in this application, the convolution of long-length signals is exchanged by products among scalars, which is also more computationally efficient.

V. CONCLUSIONS

In this article we exploited the subject of data-selective adaptive filters, and discussed its potentials to solve real-world problems. As examples of applications, we described two data-selective algorithms that can be applied to communications systems and acoustic echo cancellation in order to increase their efficiency, but data selection mechanisms can be applied to a number of applications, especially in multimedia signal processing.

ACKNOWLEDGMENT

We would like to thank CNPq, CAPES and FAPERJ for funding this work.

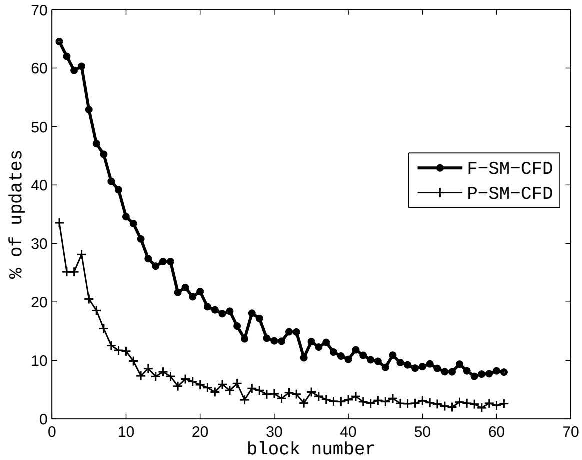

Fig. 4. Average percentage of updates in each block (computed up to last block of the smallest signal).

REFERENCES

[1] P.S.R. Diniz, *Adaptive Filtering: Algorithms and Practical Implementation*, Springer, New York, NY, 3rd Edition, 2008.

[2] S. Gollamudi, S. Nagaraj, S. Kapoor, and Y.-F. Huang, "Set-membership filtering and a set-membership normalized LMS algorithm with an adaptive step size," *IEEE Signal Processing Letters*, vol. 5, pp. 111-114, May 1998.

[3] S. Werner and P.S.R. Diniz, "Set-membership affine projection algorithm," *IEEE Signal Processing Letters*, vol. 8, pp. 231-235, Aug. 2001.

[4] L. Guo and Y.-F. Huang, "Frequency-domain set-membership filtering and its applications," *IEEE Transactions on Signal Processing*, vol. 55, pp. 1326-1338, April 2007.

[5] IEEE Std 802.11n-2009, "IEEE 802 Part 11: Wireless LAN Medium Access Control (MAC) and Physical Layer (PHY) Specifications," October 2009.

[6] IEEE Std 802.16-2009, "IEEE 802 Part 16: Air Interface for Broadband Wireless Access Systems," May 2009.

[7] 3GPP TR 36.211, "E-UTRA; physical channels and modulation," Version 9.1.0, Mar. 2010.

[8] 3GPP TR 36.101, "E-UTRA; user equipment radio transmission and reception," Version 9.8.0, Jun. 2011.

[9] Y.-P. Lin, S.-M. Phoong, P. P. Vaidyanathan, *Filter Bank Transceivers for OFDM and DMT Systems*, Cambridge Univ. Press, Cambridge, UK, 2010.

[10] J. Benesty, T. Gansler, D. R. Morgan, M. M. Sondhi, and S. L. Gay, *Advances in Network and Acoustic Echo Cancellation*, Springer, Berlin Heidelberg, Germany, 2010.

[11] H. Fastl and E. Zwicker, *Psychoacoustics: Facts and Models*, Springer, Berlin Heidelberg, Germany, 3rd Edition, 2007.

[12] A. Alcaim, J. A. Solewicz, and J. A. de Moraes, "Freqüência de ocorrência dos fones e listas de frases foneticamente balanceadas no português falado no Rio de Janeiro," *Magazine of Brazilian Telecommunications Society*, vol. 7, n. 1, pp. 23-41, December 1992 (in Portuguese).

[13] ITU-T Rec. P.800, "Methods for subjective determination of transmission quality," International Telecommunications Union, Geneva, Switzerland, 1996.

[14] E. Deruty, "Impulse Responses," available at: `http://1-1-1-1.net/pages/impulses/index.htm`, 2008.

[15] Music Technology Studio, "Impulse Responses," available at: `https://files.nyu.edu/ar137/public/research_mtechirs.html`, 2008.